EPJ Photovoltaics **8**, 80401 (2017)
www.epj-pv.org
DOI: 10.1051/epjpv/2017002

In-situ evaluation of dye adsorption on TiO_2 using QCM

Z. Besharat[1,2,a], R. Alvarez-Asencio[1,3], H. Tian[4], S. Yu[5], C.M. Johnson[1], M. Göthelid[2], and M.W. Rutland[1]

[1] KTH Royal Institute of Technology, Dept. of Chemistry, Division of Surface and Corrosion Science, 100 44 Stockholm, Sweden
[2] KTH Royal Institute of Technology, Material Physics, ICT, 164 40 Stockholm, Sweden
[3] Institute for Advanced Studies, IMDEA Nanociencia, c/o Faraday 9, Campus Cantoblanco, 28049 Madrid, Spain
[4] Uppsala University, Dept. of Chemistry, Physical Chemistry, Box 523, 751 20 Uppsala, Sweden
[5] KTH Royal Institute of Technology, Dept. of Chemistry, Fiber and Polymer Technology, 10044 Stockholm, Sweden

Received: 4 October 2016 / Received in final form: 21 January 2017 / Accepted: 24 January 2017

Abstract We measured the adsorption characteristics of two organic dyes; triphenylamine-cyanoacrylic acid (TPA-C) and phenoxazine (MP13), on TiO_2, directly in a solution based on quartz crystal microbalance (QCM). Monitoring the adsorbed amount as a function of dye concentration and during rinsing allows determination of the equilibrium constant and distinction between chemisorbed and physisorbed dye. The measured equilibrium constants are 0.8 mM^{-1} for TPA-C and 2.4 mM^{-1} for MP13. X-ray photoelectron spectroscopy was used to compare dried chemisorbed layers of TPA-C prepared in solution with TPA-C layers prepared via vacuum sublimation; the two preparation methods render similar spectra except a small contribution of water residues (OH) on the solution prepared samples. Quantitative Nanomechanical Mapping Atomic Force Microscopy (QNM-AFM) shows that physisorbed TPA-C layers are easily removed by scanning the tip across the surface. Although not obvious in height images, adhesion images clearly demonstrate removal of the dye.

1 Introduction

The climate change and finite resources of oil call for renewable non-fossil energy sources. The dye sensitized solar cells (DSSCs) is one potent solution to transform solar energy to electricity. The function is based on photo absorption and charge excitation in a dye, from where the excited electron transfers to a TiO_2 substrate [1–3]. While Ru-based dyes are commonly used, the development of pure organic dyes has also pushed their efficiencies to around 13–14% [4, 5]. Thus, the replacement of noble metal complexes with organic dyes would be possible and bring in several advantages, such as reducing production costs and increasing the environmental friendliness [6]. The output voltage from the cell is determined by the energy levels in the system; the TiO_2 pseudo-Fermi level and the redox potential of the electrolyte. The energy difference between occupied molecular orbital and unoccupied molecular orbital of the dye determines the range of absorbed wavelengths and should be matched to the solar spectrum. The current from the cell depends on the extinction coefficient of the dye, the ease of electron injection from dye to TiO_2, which depends on the adsorption geometry and the amount of dye in the excited volume. One would therefore like to maximize the amount of dye, at the same time avoid their aggregation into clusters or multilayer films, leading to reduced efficiency due to poor electron transport through the film [7–9]. Thus, the structure and density of the dye layer is crucial, and well-ordered chemisorbed monolayers turns out to be the most efficient [10].

Here, in contrast to the classical methods for measuring dye adsorption and their equilibrium constant via absorption spectroscopy, we use a fast and easy method to evaluate adsorption characteristics for on TiO_2 including the absorbed amount, equilibrium constant and presence of physisorbed aggregates or multilayers directly in solution, based on quartz crystal microbalance (QCM-D) in a liquid flow cell. Two different dyes Triphenylamin-cyanoacrylic acid (TPA-C) and Phenoxazine (MP13), which has also been used in other research group [11, 12] are used. To support the evaluation we also performed X-ray photoelectron spectroscopy (XPS) on dried liquid phase prepared dye layers and on vacuum sublimated monolayer films on a TiO_2 single crystal. The mechanical properties of the dye film were investigated by atomic force microcopy (AFM).

[a] e-mail: besharat@kth.se

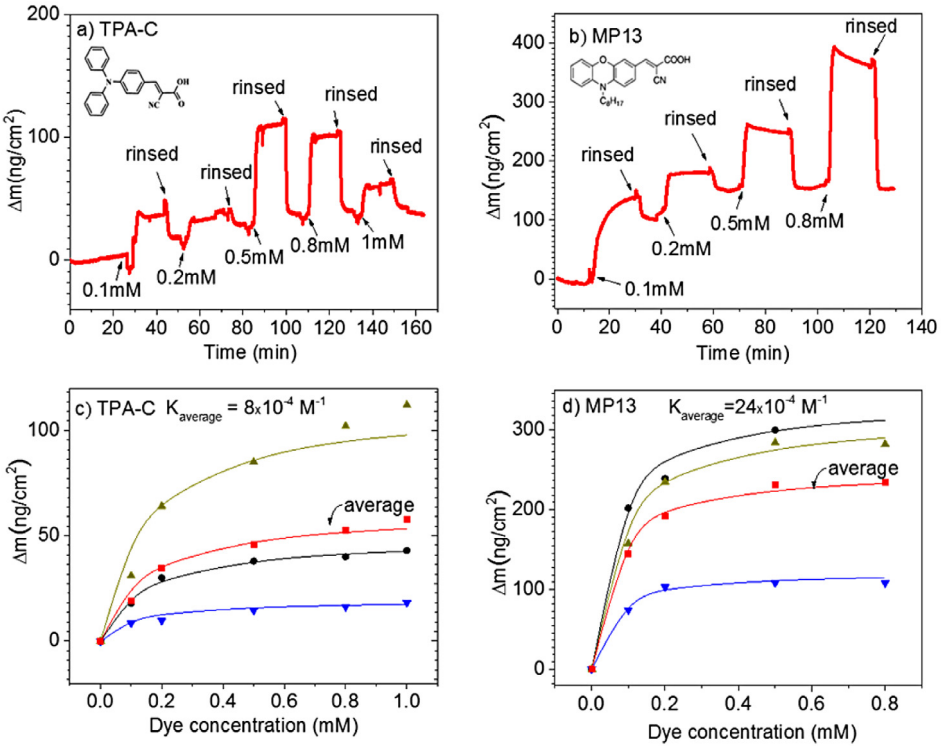

Fig. 1. (a, b) Shows adsorbed mass of dye from solution at different concentration vs. time (a) TPA-C (b) MP13. (c, d) Shows the chemisorbed mass vs. concentration for TPA-C and MP13 respectively. The red curves with square symbols in (c) and (d) are averages of the three runs.

2 Experimental

Triphenylamin-cyanoacrylic acid (TPA-C), see inset in Figure 1, was prepared according to Kitamura et al. [13]. Phenoxazine (MP13), see inset in Figure 1b, was prepared following Karlsson et al. [14]. All solutions were prepared with ethanol (99.9%) from VWR International. QCM crystals with a 25 nm thick mixture of rutile and anatase polycrystalline TiO_2 film on top of AT cut quartz crystal (QSX 999 TiO_2) were used as substrate in the QCM-D and XPS measurements. For AFM we used a rutile $TiO_2(001)$ single crystal (Surface Preparation Laboratory, The Netherlands). For the vacuum sublimated TPA-C films we used a rutile $TiO_2(110)$ crystal (Surface Preparation Laboratory, The Netherlands) cleaned in vacuum by cyclic Ar-sputtering and heating to 550 °C. TPA-C sublimation was done in UHV from a well outgassed quartz tube heated by a W-filament [15].

For cleaning the TiO_2 QCM substrates, they were immersed in the chromosulfuric acid for 20 min and rinsed several times with adequate amounts of Milli-Q water. The crystals were kept in ethanol until used. Freshly cleaned and dye sensitized TiO_2 QCM-D samples (located in 0.5 mm dye solution for 3 h and rinsed by ethanol after) were prepared for the XPS measurements too. $TiO_2(001)$ surfaces were heated at 650 °C and ultrasonically cleaned in ethanol for 30 min followed by Milli-Q water for 30 min, and finally UV-ozone treated (ProCleaner, BioForce Nanoscience) for 20 min. Afterwards the surface was immediately used in the AFM liquid cell. The 0.5 mM TPA-C dye was injected into the liquid cell and kept there for 3 h.

The adsorbed amount of dye on the QCM-TiO_2 samples was measured with a Q-Sense E4 QCM-D (Biolin Scientific, Sweden), in a flow cell with a flow rate kept at 150 μL min^{-1} via a peristaltic pump (Ismatec IPC-N4). The principle of QCM-D is based on the shift of an electro-acoustic resonance frequency (Δf) by loading of mass. The change in the resonant frequency of the oscillating crystal is proportional to the adsorbed mass on the surface, according to the Sauerbrey equation (1) [16], as long as energy dissipation $\Delta D/\Delta f < 4 \times 10^{-7}$ Hz^{-1} for a 5 MHz crystal [17],

$$(1)\ \Delta m = -C\frac{1}{n}\Delta f \qquad C = 17.7 \text{ ng cm}^{-2} \text{ Hz}^{-1}$$
$$n = \text{overtones}. \tag{1}$$

In this work, dissipation was small even at the high concentrations and the Sauerbrey equation is applicable.

Photoemission measurements were done at beamline I311 at MAX-lab in Lund. Photons in the range of 50–1500 eV were produced by an undulator and selected by a modified Zeiss SX-700 plane grating monochromator. Electron spectra were recorded, in normal emission, by a Scienta SES200 electron analyzer. The base pressure in the analysis chamber was 1×10^{-10} mbar. A preparation chamber equipped with low-energy electron diffraction (LEED) and sample cleaning was connected to the analysis chamber. For each sample, an overview spectrum was recorded,

followed by detailed high resolution spectra. All spectra were normalized to the background (the intensity at the lower binding energy side). The energy scale is with respect to the Fermi level of a metallic clip in contact with the sample. Curve fitting was done using Voigt functions and a linear background with the fitxps2 program.

Nanometer resolution images containing surface topography and surface material properties have been obtained using and AFM Multimode, Nanoscope V, (Bruker®, Santa Barbara, CA), which operates in PeakForce® QNM mode. In PeakForce® the scanner oscillates with a frequency in the range of 1–2 kHz, making intermittent contact with a cantilever tip. As the surface is scanned, the cantilever deflection and piezo position are collected by feedback system. These data are afterwards converted to force vs. distance curves using the optical level sensitivity and spring constants of the cantilever which provide not only topographic information but surface material properties [18–21]. These measurements were performed in 0.5 mM dye solution for 3 h in a standard tapping liquid cell "MTFML" (Bruker®, Santa Barbara, CA) where a liquid volume of around 0.1 mL can be contained. Silicon tips HQ:NSC19/No Al, MikroMasch (Estonia) with a nominal tip radius of 8 nm and nominal spring constant of 0.5 N m^{-1} were used for all the measurements. The cantilevers were calibrated according to the procedures described in references [22,23], respectively. Experiments were performed with a constant force of 1.5 nN, scan sizes of 10×10 μm^2, 3×3 μm^2 and 1×1 μm^2, 1 Hz scan rate and image resolution of 256×256 pixels. All AFM data were processed and analyzed using the NanoScope Analysis software (version 1.40, Bruker Corporation). The bow and tilt corrections of the topography images were performed applying a second order polynomial flattening algorithm. The liquid cell and all of the its accessories were cleaned by keeping them in the 2% Hellmanex (Hellma GmbH) solution for 1 h and rinsed several times with Milli-Q water. The experiments were run in the dye solution in order to keep physisorbed layer on top of the surface.

3 Results and discussion

Figure 1 shows the adsorbed mass on a TiO_2 QCM-D sensor in dye solutions at different concentration from 0.1 mM to 1 mM. The graph in Figure 1a is from TPA-C and Figure 1b from MP13. Injections of dye solution, for each concentration, are indicated by arrows in the figure, separated by 10 min rinsing with pure ethanol to wash away physisorbed dye. The higher plateaus in the graphs correspond to the combined mass of physisorbed and chemisorbed dye at equilibrium, whereas the mass after rinsing represents the chemisorbed mass only. The chemisorbed mass follows a smooth trend, as presented in Figures 1c and 1d. The separate graphs are data from three separate runs on each dye, using different TiO_2 QCM-D sensors from the same batch. The red curves with square symbols in Figures 1c and 1d are averages of the three runs. The chemisorbed and physisorbed masses and their ratio at different concentration are shown in Table 1.

Table 1. Chemisorbed and physisorbed masses and their ratio at different concentrations.

Concentration		A: Average physisorbed mass	B: Average chemisorbed mass	A/B
TPAC	0.1	37	27	1.37
	0.2	38	33	1.15
	0.5	111	48	2.31
	0.8	101	52	1.94
	1	66	53	1.24
MP13	0.1	223	173	1.29
	0.2	243	203	1.20
	0.5	374	226	1.65
	0.8	526	226	2.33

The measured masses are indicated by dots and the solid lines are fits using the Langmuir equation below (2); c is the concentration is the solution, K is the equilibrium constant, θ is the occupied fraction of adsorption sites at each concentration and θ_{max} is the maximum coverage, when all adsorption sites are filled, on that particular sample. Clearly θ_{max} varies between different sensors. This is due to variations in the active surface area and surface roughness, which will affect the θ_{max}, but the K-values are comparable. From the fit we obtain the equilibrium constants; 0.8 mM^{-1} for TPA-C and 2.4 mM^{-1} for MP13.

$$\theta = \theta_{max} \frac{Kc}{1 + Kc}. \quad (2)$$

The adsorbed mass for each sensor is different (Tab. 1 and Figs. 1a and 1b) which is due to the active surface site of each sensor. The active sites in sensors are not identical and that will influence on the amount of adsorption and tolerance the adsorb mass in each individual sensor. The morphology and surface roughness will effect on the adsorption amount on the surface [24]. However, by considering the Langmuir adsorption, principally, all active site will be filled with adsorbate and consequently give similar equilibrium constant of each dye on all sensors. Despite the rather large variations in the measured adsorbed masses, it is clear that the chemisorbed mass of MP13 is more than a factor of 3 times larger than the adsorbed TPA-C mass. The molecular mass of MP13 is only 1.11 times higher than the molecular mass of TPA-C, and we conclude that MP13 forms a considerably denser layer than TPA-C, in line with the smaller equilibrium constant for TPA-C than for MP13.

Rinsing removes physisorbed dye and has proven to increase film quality and stability [25], since charge transfer from physisorbed dye to TiO_2 will not be as efficient as when the dye is chemisorbed [7,26,27]. The amount of physisorbed MP13 increases smoothly with solution concentration, whereas for TPA-C the washed-off mass varies less predictably. Layer appears smoother, and the adsorbed amount is higher than T-PAC. This can be explained by the dye structure and the existence of alkyl chain. For the Z907 dye, it was shown by Harms and co-workers, that an

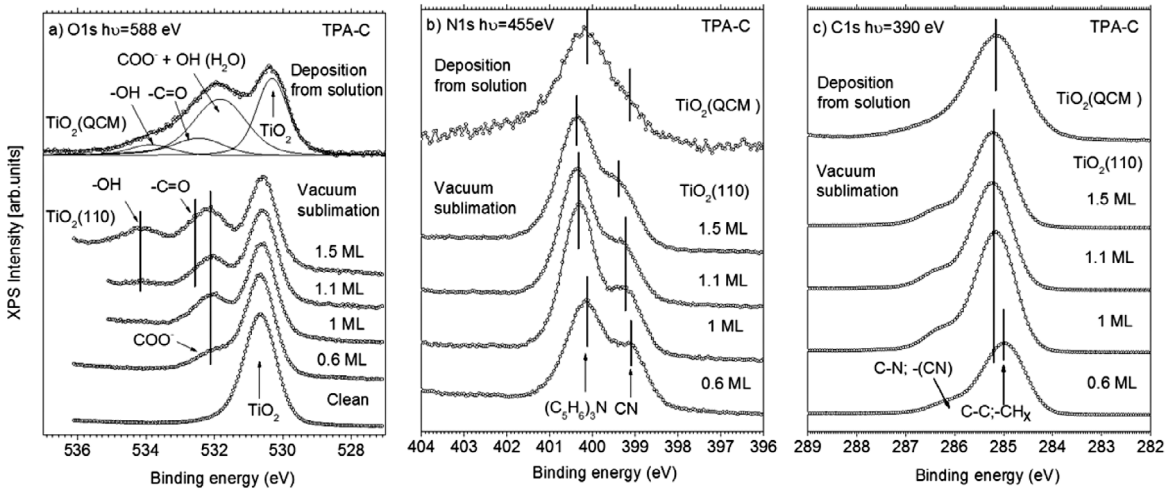

Fig. 2. O1, N1s, and C1s core level spectra from TPA-C on TiO2. Photon energies are indicated in the figure.

alkyl chain increase order within the monolayer [28]. Moreover, the interaction of dyes in the monolayer which could be affected by their structure influence on the equilibrium constant [29].

Photoemission from O1s, C1s and N1s from TPA-C layers on TiO_2 is shown in Figure 2. Each panel contains spectra from vacuum sublimated films on $TiO_2(110)$ at different coverages and in the top the corresponding spectrum from the TiO_2 QCM-D sensor. Upon adsorption of TPA-C, the OH is deprotonated and the molecule binds with both oxygens to $TiO_2(110)$ and the triphenyl group pointing away from the surface, resulting in one strong O1s component (COO^-), at 1.45 eV higher binding energy than the O1s peak of TiO_2 [15]. At coverages above 1 monolayer a new component, (-OH), appears around 534 eV, which was assigned to oxygen in the OH part of second layer TPA-C molecules, not bound directly to the surface [15]. In the second layer the carboxylic group is not deprotonated leading to two separate O1s components (-C = O) and (-OH) with similar intensity, separated by 1.66 eV [15].

O1s from the solution-made TPA-C film has a different shape and is broader. Despite only three peaks are visible to the eye, we make a numerical fit with the four components based on the results from the vacuum sublimated samples. The presence of (-OH) indicates TPA-C without bond between carboxyl group and TiO_2, for which we also add (-C = O), with the same intensity as (-OH). The (COO^-) peak is stronger than expected compared to the sublimated film, but since the sample was transported in air water will adsorb. Water is not expected to remain on the surface at room temperature in UHV [30], but it can remain as OH on the TiO_2 surface. O1s for OH on TiO_2 appears at 1.6 eV higher binding energy than O1s in TiO_2 [31], very close to (COO^-). The O1s results thus indicates a film dominated by TPA-C bound to TiO_2, with some water residues, but also TPA-C without carboxyl-TiO_2 bond.

N1s comprises two components, marked CN and $(C_5H_6)_3N$, from the two nitrogen atoms in the molecule. The relative intensity of the triphenyl contribution is higher, which was explained as an effect of the adsorption geometry with the carboxylic part binding to the surface leading to a damped signal from that nitrogen. N1s from the TiO_2 QCM-D sample, in the top of the panel, is very similar to spectra from the sublimated films. However, it is not possible from these spectra to determine the coverage.

There are three groups of carbon atoms within the TPA-C molecule; C binding only to other C and to H, C binding to O and C binding to N. C1s comprises one main component and one smaller shoulder on the high binding energy side. The main C1s is related to C without bonds to O or N, whereas the spectral shoulder represents the four carbon atoms binding to N [15]. One could also expect a contribution from the single C atom binding to two oxygens, but the intensity is very low here. The C1s from the QCM-D sample is broader than from the sublimated films, which can be due to disorder, impurities or both. One could perhaps suspect ethanol residues, but C1s from ethanol has two clearly separated peaks [32], and we rule out ethanol. Water, or rather OH, is not directly visible in the C1s spectrum, but its presence will affect the electronic environment around the carbon atoms and could potentially broaden the spectrum.

We thus conclude that the TPA-C film made from solution and rinsing results in a dye layer dominated by TPA-C firmly adsorbed to TiO_2 together with OH from water. But also a small amount of ad-layer dye not in contact with the surface, indicating island growth.

PeakForce® QNM was used to investigate a physisorbed TPA-C film, formed at 0.5 mM concentration, on $TiO_2(100)$. Figure 3 shows 10×10 μm^2 images (height and adhesion) obtained after scanning the surface first 1×1 μm^2, then 3×3 μm^2 and finally 10×10 μm^2. The central part of height image is not obviously different from the peripheral parts, whereas the adhesion image clearly shows a difference between previously scanned areas and untouched areas. Adhesion reflects a difference in the tip-surface interaction. Line profiles, from the blue lines in the images, are shown in Figures 3c and 3d.

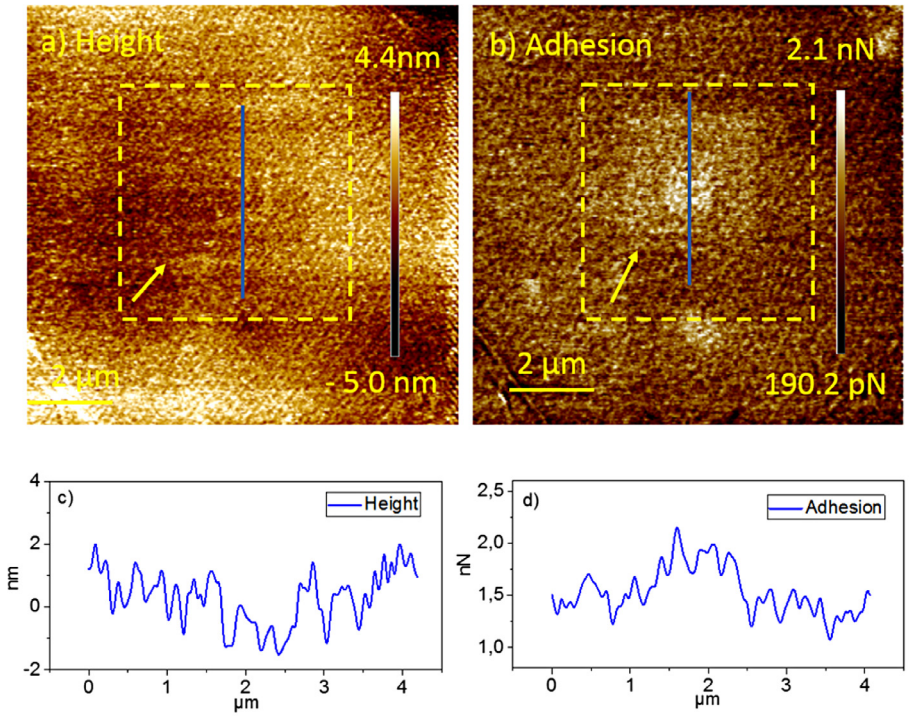

Fig. 3. PeakForce AFM images of TiO_2 surface after ascending order of scans area from 1×1 μm^2 till 10×10 μm^2 in 0.5 mM TPA-C dye solution after 3 h (a) height (b) adhesion (c) height profile and (d) adhesion profile.

According to the height profile in Figure 3c, the removed layer after two successive scans is approximately 1 to 2 nm thick, which is in the order of molecular dimensions. The QCM-D results indicated a considerable amount of physisorbed mass before rinsing. Scanning the surface with a force of 1.5 nN is enough to remove the physisorbed dye layer.

4 Conclusions

In this work, we have measured dye adsorption on TiO_2 using a QCM-D sensor in dye solutions of TPA-C and MP13. From fitting to the Langmuir adsorption model values for equilibrium constants were extracted; 0.8 mM^{-1} for TPA-C and 2.4 mM^{-1} for MP13. MP13 adsorbs in larger amounts than TPA-C, which could be due to a better packing structure for MP13 than TPA-C dye. Vacuum sublimated TPA-C films and dried films made from solution display very similar XPS results, except a small amount of water residues on the wet prepared samples due to transport in air. TPA-C films are concluded to be in the monolayer coverage regime, but with a small amount of dye molecules that are not in contact with the surface. Physisorbed dye can easily be removed by an AFM tip.

The financial support from the Swedish Research Council (VR) is gratefully acknowledged. S.Y. acknowledges the financial support from Knut and Alice Wallenberg Foundation. The authors thank Prof Licheng Sun for valuable discussions.

References

1. M. Grätzel, J. Photochem. Photobiol. C: Photochem. Rev. **4**, 145 (2003)
2. Y. Tachibana, J.E. Moser, M. Grätzel, D.R. Klug, J.R. Durrant, J. Phys. Chem. **100**, 20056 (1996)
3. M. Grätzel, Inorganic Chem. **44**, 6841 (2005)
4. S. Mathew, A. Yella, P. Gao, R. Humphry-Baker, F.E. CurchodBasile, N. Ashari-Astani, I. Tavernelli, U. Rothlisberger, K. NazeeruddinMd, M. Grätzel, Nat. Chem. **6**, 242 (2014)
5. K. Kakiage, Y. Aoyama, T. Yano, K. Oya, J.-I. Fujisawa, M. Hanaya, Chem. Commun. **51**, 15894 (2015)
6. H. Tian, X. Yang, R. Chen, R. Zhang, A. Hagfeldt, L. Sun, J. Phys. Chem. C **112**, 11023 (2008)
7. A. Hagfeldt, G. Boschloo, L. Sun, L. Kloo, H. Pettersson, Chem. Rev. **110**, 6595 (2010)
8. J.R. Mann, M.K. Gannon, T.C. Fitzgibbons, M.R. Detty, D.F. Watson, J. Phys. Chem. C **112**, 13057 (2008)
9. L. Ellis-Gibbings, V. Johansson, R.B. Walsh, L. Kloo, J.S. Quinton, G.G. Andersson, Langmuir **28**, 9431 (2012)
10. H.A. Harms, N. Tetreault, V. Gusak, B. Kasemo, M. Gratzel, Phys. Chem. Chem. Phys. **14**, 9037 (2012)
11. T. Marinado, K. Nonomura, J. Nissfolk, M.K. Karlsson, D.P. Hagberg, L. Sun, S. Mori, A. Hagfeldt, Langmuir **26**, 2592 (2010)
12. H. Tian, X. Yang, J. Cong, R. Chen, J. Liu, Y. Hao, A. Hagfeldt, L. Sun, Chem. Commun. **2009**, 6288 (2009)
13. T. Kitamura, M. Ikeda, K. Shigaki, T. Inoue, N.A. Anderson, X. Ai, T. Lian, S. Yanagida, Chem. Mater. **16**, 1806 (2004)
14. K.M. Karlsson, X. Jiang, S.K. Eriksson, E. Gabrielsson, H. Rensmo, A. Hagfeldt, L. Sun, Chem.-A Eur. J. **17**, 6415 (2011)

15. S. Yu, S. Ahmadi, M. Zuleta, H. Tian, K. Schulte, A. Pietzsch, F. Hennies, J. Weissenrieder, X. Yang, M. Göthelid, J. Chem. Phys. **133**, 224704 (2010)
16. G. Sauerbrey, Z. Phys. **155**, 206 (1959)
17. I. Reviakine, D. Johannsmann, R.P. Richter, Anal. Chem. **83**, 8838 (2011)
18. F. Rico, C. Su, S. Scheuring, Nano Lett. **11**, 3983 (2011)
19. K. Sweers, K. van der Werf, M. Bennink, V. Subramaniam, Nanoscale Res. Lett. **6**, 270 (2011)
20. M. Sababi, J. Kettle, H. Rautkoski, P.M. Claesson, E. Thormann, Appl. Mater. Interfaces **4**, 5534 (2012)
21. K. Sweers, K. van der Werf, M. Bennink, V. Subramaniam, Nanoscale Res. Lett. **6**, 1 (2011)
22. H.J. Butt, M. Jaschke, Nanotechnology **6**, 1 (1995)
23. E. Thormann, T. Pettersson, P.M. Claesson, Rev. Sci. Instrum. **80**, 093701 (2009)
24. L.B. Roberson, M.A. Poggi, J. Kowalik, G.P. Smestad, L.A. Bottomley, L.M. Tolbert, Coordination Chem. Rev. **248**, 1491 (2004)
25. V. Gusak, E. Nkurunziza, C. Langhammer, B. Kasemo, J. Phys. Chem. C **118**, 17116 (2014)
26. F. Hirose, K. Kuribayashi, M. Shikaku, Y. Narita, Y. Takahashi, Y. Kimura, M. Niwano, J. Electrochem. Soc. **156**, B987 (2009)
27. T. Luitel, F.P. Zamborini, Langmuir **29**, 13582 (2013)
28. K. Voïtchovsky, N. Ashari-Astani, I. Tavernelli, N. Tétreault, U. Rothlisberger, F. Stellacci, M. Grätzel, H.A. Harms, Appl. Mater. Interfaces **7**, 10834 (2015)
29. M. Pastore, T. Etienne, F. De Angelis, J. Mater. Chem. C **4**, 4346 (2016)
30. M.B. Hugenschmidt, L. Gamble, C.T. Campbell, Surf. Sci. **302**, 329 (1994)
31. L.Q. Wang, D.R. Baer, M.H. Engelhard, A.N. Shultz, Surf. Sci. **344**, 237 (1995)
32. H. Idriss, E.G. Seebauer, J. Molecular Catalysis A: Chemical **152**, 201 (2000)

Cite this article as: Z. Besharat, R. Alvarez-Asencio, H. Tian, S. Yu, C.M. Johnson, M. Göthelid, M.W. Rutland, In-situ evaluation of dye adsorption on TiO_2 using QCM, EPJ Photovoltaics **8**, 80401 (2017).